JOURNAL OF BACTERIOLOGY, Mar. 1991, p. 1711–1721
0021-9193/91/051711-11$02.00/0

Vol. 173, No. 5

Structure of *Escherichia coli* K-12 *miaA* and Characterization of the Mutator Phenotype Caused by *miaA* Insertion Mutations

DENNIS M. CONNOLLY[1] AND MALCOLM E. WINKLER[2]*

Department of Molecular Biology, Northwestern University Medical School, Chicago, Illinois 60611,[1] and Department of Microbiology, University of Texas Medical School, Houston, Texas 77030[2]

Received 6 August 1990/Accepted 10 December 1990

Previously, we reported several unusual relationships between the 2-methylthio-N^6-(Δ^2-isopentenyl)adenosine-37 (ms^2i^6A-37) tRNA modification and spontaneous mutagenesis in *Escherichia coli* K-12 (D. M. Connolly and M. E. Winkler, J. Bacteriol. 171:3233–3246, 1989). To confirm and extend these observations, we determined the structure of *miaA*, which mediates the first step of ms^2i^6A-37 synthesis, and characterized the *miaA* mutator phenotype. The most likely translation start of *miaA* overlaps the last two codons of *mutL*, which encodes a protein required for methyl-directed mismatch repair. This structural arrangement confirms that *miaA* and *mutL* are in the same complex operon. The *miaA* gene product, Δ^2-isopentenylpyrophosphate transferase, shows extensive homology with the yeast *MOD5* gene product, and both enzymes contain a substrate binding site found in farnysyl pyrophosphate synthetase and a conserved putative ATP/GTP binding site. Insertions in *miaA* cause exclusively GC→TA transversions, which contrasts with the GC→AT and AT→GC transitions observed in *mutL* mutants. To correlate the absence of the ms^2i^6A-37 tRNA modification directly with the mutator phenotype, we isolated a unique suppressor of a leaky *miaA*(ochre) mutation. The *miaD* suppressor mapped to 99.75 min, restored the ms^2i^6A-37 tRNA modification to *miaA*(ochre) mutants, and abolished the *miaA* mutator phenotype. We speculate that *miaD* causes a decrease in ms^2i^6A-37 tRNA demodification or an increase in *miaA* gene expression but not at the level of operon transcription. Together, these observations support the idea that the ms^2i^6A-37 tRNA modification acts as a physiological switch that modulates spontaneous mutation frequency and other metabolic functions.

The hypermodified, hydrophobic 2-methylthio-N^6-(Δ^2-isopentenyl)adenosine (ms^2i^6A) modification (Fig. 1) occurs 3′ to the anticodon in tRNA species that read codons beginning with U residues (6, 7). The final modification consists of two parts, which are added sequentially to adenosine-37 (A-37) of appropriate tRNA species (1, 9, 22). The first step in ms^2i^6A-37 biosynthesis is the addition of a Δ^2-isopentenyl(dimethylallyl) group to the N^6 nitrogen of adenosine (Fig. 1, left). This reaction is catalyzed in *Escherichia coli* by the *miaA* gene product, Δ^2-isopentenylpyrophosphate transferase (5, 13, 15, 20, 48) and provides a metabolic link between isoprenoid biosynthesis and tRNA function. In *Saccharomyces cerevisiae*, the analogous enzyme to MiaA is Mod5, which has been structurally characterized by Hopper, Martin, and their coworkers (18, 32). After i^6A-37 is formed in *E. coli*, cysteine serves as a thio donor in an iron-dependent reaction, and *S*-adenosyl-l-methionine is used as a methyl donor to complete the ms^2i^6A-37 modification (Fig. 1, right) (22, 25). These last two steps are not well characterized, but it seems likely that they occur sequentially with methyl transfer following thiolation (1, 22). The activities that catalyze methylthio formation are designated MiaB (thiolation) and MiaC (methyl transfer), but it is unknown whether they are separate enzymes or contained in a bifunctional protein.

The degree of A-37 tRNA modification has been postulated as playing a role in the bacterial cell response to certain environmental stresses (9, 11, 15, 21). In particular, iron limitation causes undermodification of ms^2i^6A-37 to i^6A-37 (Fig. 1, middle), which in turn causes increased aromatic amino acid and enterochelin biosynthesis and aromatic amino acid transport (9–11). Mechanisms that couple gene expression to translation, such as attenuation, probably mediate some of the changes in gene expression caused by tRNA undermodification, because undermodified tRNA molecules exhibit altered translation properties compared with fully modified tRNA (8, 9, 21, 24, 34, 48).

There are several unusual relationships among the *miaA* gene, ms^2i^6A-37 tRNA modification, and spontaneous mutagenesis in *E. coli* (15). Using genetic approaches and in vivo transcript analysis, we recently showed that *miaA* is most likely a downstream gene in a complex operon with *mutL* and an unknown gene, which encodes a 47-kDa polypeptide. The *mutL* gene product is required for methyl-directed mismatch repair (26, 27, 31, 35), and lesions in *mutL* result in a distinct mutator phenotype (14, 39). We also showed that insertion mutations in *miaA* cause a context-dependent mutator phenotype with a spectrum that seemed to be different from the one displayed by *mutL* mutants (15). Depending on the mutational event scored, the effect of *miaA* lesions on spontaneous mutation frequency ranged from being only slightly less than [29-fold versus 45-fold for reversion of a *lacZ*(UGA) allele] to being significantly less than (5-fold versus 1,300-fold for resistance to nalidixic acid) that of *mutL* mutations (15). Furthermore, limitation of $miaA^+$ bacteria for iron, which results in undermodification to i^6A-37 (Fig. 1), resulted in an increase in spontaneous mutation frequency. Finally, we found that *miaA* and possibly *mutL* transcription was induced significantly by the mismatch mutagen, 2-aminopurine (15). Together, these results support the notion that complex operons organize metabolically related genes whose primary functions appear to be completely different. The results are also consistent

* Corresponding author.

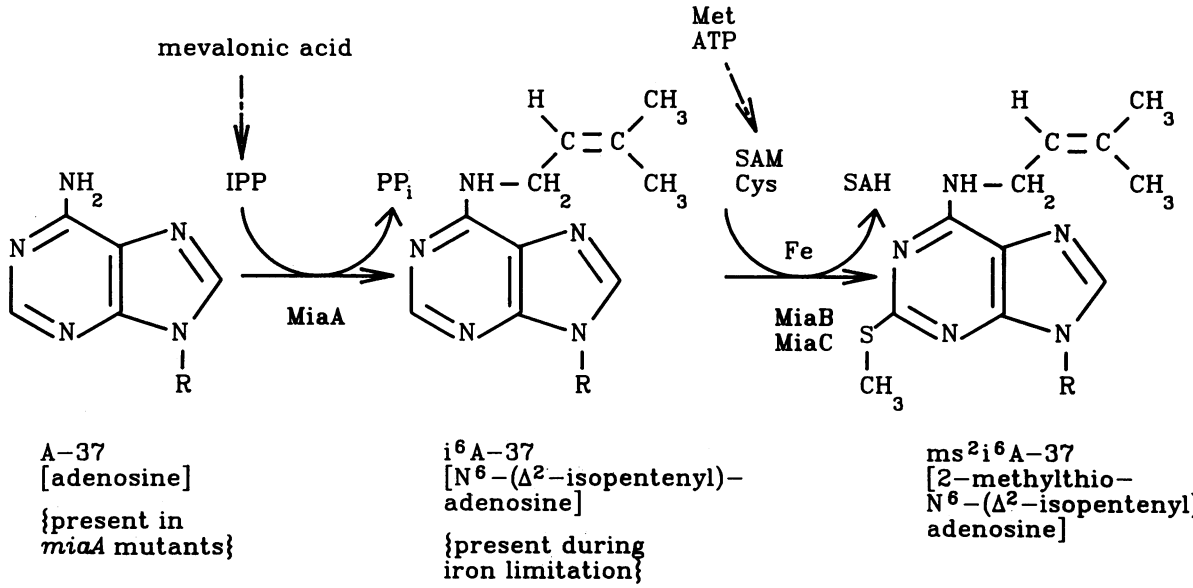

FIG. 1. Biosynthesis of ms^2i^6A at position 37 in *E. coli* tRNA species that read codons starting with U. The first step is catalyzed by the *miaA* gene product, tRNA Δ^2-isopentenylpyrophosphate (IPP) transferase, which is analogous to yeast Mod5 and shares homology with prenyl synthetases (see Results). Cysteine (Cys) and *S*-adenosylmethionine (SAM) are then used as thio and methyl donors by activities designated MiaB and MiaC, respectively. The reaction performed by MiaB is iron (Fe) dependent. SAH, *S*-Adenosylhomocysteine.

with the idea that mechanisms exist to increase spontaneous mutation frequency when cells need to adapt to environmental stress (19, 45).

In this report, we confirm and extend the above relationships between ms^2i^6A-37 tRNA modification and spontaneous mutagenesis. The DNA sequence of *miaA* establishes that *miaA* and *mutL* are indeed adjacent and probably overlap. Comparison of *E. coli* MiaA and yeast Mod5 shows a high degree of conservation but suggests that Mod5 contains an additional domain at its carboxyl terminus. The mutation spectrum of *miaA* insertion mutants was further characterized and is completely different from that of *mutL* mutants. Finally, a novel suppressor mutation of *miaA* (ochre) mutations was isolated that restores the ms^2i^6A-37 tRNA modification. Insertion in this new gene, which we designated *miaD*, possibly decreases tRNA demodification or increases posttranscriptional expression of the *miaA* gene. Restoration of the ms^2i^6A-37 tRNA modification in *miaA*(ochre) *miaD* double mutants reduces the spontaneous mutation frequency back to the $miaA^+$ level and confirms that the increased mutation frequency found in *miaA* mutants is directly attributable to lack of the ms^2i^6A-37 tRNA modification.

MATERIALS AND METHODS

Materials. Restriction endonucleases, enzymes used in cloning, and DNA polymerase I large (Klenow) fragment were purchased from New England BioLabs, Inc. (Beverly, Mass.). Biochemicals and antibiotics were from United States Biochemicals Corp. (Cleveland, Ohio), including Sequenase DNA polymerase, and Sigma Chemical Co. (St. Louis, Mo.), including bacterial alkaline phosphatase type III. Culture media were from Difco Laboratories (Detroit, Mich.). [α-^{32}P]dCTP (≈800 Ci/mmol) was from Amersham Corp. (Arlington Heights, Ill.). NACS prepac columns were from Bethesda Research Laboratories, Inc. (Gaithersburg, Md.). Nineteen-mers used as primers for DNA sequencing were synthesized by Biosis, Inc. (Woodlands, Tex.).

Bacterial strains, media, and mapping. Bacterial strains are described in Table 1. Markers were moved between strains by generalized transduction with P1 *kc* bacteriophage (30). Mini-Tn*10*(Km^r) chromosomal insertions were introduced from lambda phage 1105 (mini-*kan*) as described previously (44). Bacteria were routinely grown in LB medium supplemented with 30 μg of L-Cys per ml (designated LBC) and in Vogel-Bonner minimal (E) medium supplemented with 0.4% (wt/vol) α-D-glucose, 2 μg of thiamine per ml, and 10^{-5} M $FeSO_4$ (designated MMG [17]). Mapping of *miaD*::mini-Tn*10*(Km^r) was accomplished by using the Hfr and transduction (Tc^r) marker set developed by Singer et al. (41). Rapid, preliminary Hfr mapping localized *miaD* to 70 to 100 min. More exact transduction mapping is presented in the Results.

Phenotypic characterizations and reversion tests. Reversion of *lacZ*(UGA) and *trpA46PR9* was measured as described before (15). Reversion of the Cupples-Miller tester strains was measured as described in the table footnotes, figure legends, and reference 16. In each case, a control was included to access loss of the F′ *lac-proB*$^+$ episome by measuring CFU on MMG. Su^+9 suppressor tRNA function was assessed in the DEV15 *lacZ*(UGA) background by formation of green colonies on eosin-methylene blue agar containing 0.4% (wt/vol) lactose as described previously (15). Modified bases in total cellular RNA were analyzed by high-performance liquid chromatography (HPLC) as described before (15).

DNA sequence determination and *miaA* transcript analysis. DNA sequence determinations were completed on both strands with all overlaps. *Stu*I-*Bam*HI and *Bam*HI-*Kpn*I restriction fragments extending upstream or downstream from *miaA* (Fig. 2, right) were each cloned into M13mp18 and M13mp19 phage. The DNA sequence surrounding the

TABLE 1. Bacterial strains[a]

Strain	Genotype[b]	Source or reference
CC101	P90C [*ara* Δ(*lac-proB*)XIII (F′ *lacIZ proB*$^+$)] (AT→CG tester strain)	J. Miller (16)
CC102	Similar to CC101 (GC→AT tester strain)	J. Miller (16)
CC103	Similar to CC101 (GC→CG tester strain)	J. Miller (16)
CC104	Similar to CC101 (GC→TA tester strain)	J. Miller (16)
CC105	Similar to CC101 (AT→TA tester strain)	J. Miller (16)
CC106	Similar to CC101 (AT→GC tester strain)	J. Miller (16)
DEV14	Hfr *thi relA spoT lacZ*(UAA)	D. Elseviers (36)
DEV15	Hfr *thi relA spoT lacZ*(UGA)	D. Elseviers (36)
DEV15 *miaA*	DEV15 *miaA*(ochre) = *trpX*	D. Elseviers (36)
DEV15 *su*$^+$*9*	DEV15 *su*$^+$*9*	D. Elseviers (36)
DEV15 *su*$^+$*9 miaA*	DEV15 *su*$^+$ *9 miaA*(ochre)	D. Elseviers (36)
DEV15 *miaA*::Tn*10*	DEV15 *miaA*::Tn*10*(Tc^r)	D. Elseviers (36)
JM105	*thi rpsL* Δ(*lac-proAB*) (F′ *traD36 proAB lacI*^{q}ZΔM15)	J. Messing (46)
NU426[c]	W3110 *sup*(Am) prototroph (probably W1485E)	C. Yanofsky collection
NU743[d]	NU426 *miaA*::KmSma	Laboratory collection (15)
NU744[d]	NU426 *mutL*::KmΔMlu	Laboratory collection (15)
NU753	W3310 *tna-2 trpA46PR9* Δ*lacU169 miaA*::KmSma	Laboratory collection (15)
NU814	W3110 *tna-2* prototroph (*sup*^{0})	C. Yanofsky collection
NU1505	CC101 *miaA*::KmSma	CC101 × P1 *kc* (NU743)
NU1506	CC101 *mutL*::KmΔMlu	CC101 × P1 *kc* (NU744)
NU1508	CC102 *miaA*::KmSma	CC102 × P1 *kc* (NU743)
NU1509	CC102 *mutL*::KmΔMlu	CC102 × P1 *kc* (NU744)
NU1511	CC103 *miaA*::KmSma	CC103 × P1 *kc* (NU743)
NU1512	CC103 *mutL*::KmΔMlu	CC103 × P1 *kc* (NU744)
NU1514	CC104 *miaA*::KmSma	CC104 × P1 *kc* (NU743)
NU1515	CC104 *mutL*::KmΔMlu	CC104 × P1 *kc* (NU744)
NU1517	CC105 *miaA*::KmSma	CC105 × P1 *kc* (NU743)
NU1518	CC105 *mutL*::KmΔMlu	CC105 × P1 *kc* (NU744)
NU1520	CC106 *miaA*::KmSma	CC106 × P1 *kc* (NU743)
NU1521	CC106 *mutL*::KmΔMlu	CC106 × P1 *kc* (NU744)
NU1552	DEV15 *su*$^+$*9 miaA*(ochre) *miaD*::mini-Tn*10*(Km^r)	Random mini-Tn*10* jumps
NU1846	NU814 *miaD*::mini-Tn*10*(Km^r)	NU814 × P1 *kc* (NU1552)
NU1847	DEV14 *miaD*::mini-Tn*10*(Km^r)	DEV14 × P1 *kc* (NU1552)
NU1848	NU1886 *miaD*::mini-Tn*10*(Km^r)	NU1886 × P1 *kc* (NU1552)
NU1849	CC101 *miaD*::mini-Tn*10*(Km^r)	CC101 × P1 *kc* (NU1552)
NU1850	CC102 *miaD*::mini-Tn*10*(Km^r)	CC102 × P1 *kc* (NU1552)
NU1851	CC103 *miaD*::mini-Tn*10*(Km^r)	CC103 × P1 *kc* (NU1552)
NU1852	CC104 *miaD*::mini-Tn*10*(Km^r)	CC104 × P1 *kc* (NU1552)
NU1853	CC105 *miaD*::mini-Tn*10*(Km^r)	CC105 × P1 *kc* (NU1552)
NU1854	CC106 *miaD*::mini-Tn*10*(Km^r)	CC106 × P1 *kc* (NU1552)
NU1879	DEV15 *miaA*(ochre) *miaD*::mini-Tn*10*(Km^r)	DEV15 *miaA* × P1 *kc* (NU1552)
NU1880	DEV15 *miaA*::Tn*10*(Tc^r) *miaD*::mini-Tn*10*(Km^r)	DEV15 *miaA*::Tn*10* × P1 *kc* (NU1552)
NU1885	DEV15 *miaD*::mini-Tn*10*(Km^r)	DEV15 × P1 *kc* (NU1552)
NU1886	W3110 *trpR miaA*(ochre) *lacZU118*(UAA)	C. Yanofsky collection
NU1887	DEV15 *su*$^+$*9 miaD*::mini-Tn*10*(Km^r)	DEV15 *su*$^+$*9* × P1 *kc* (NU1552)
NU1888	DEV15 *su*$^+$*9 miaA*(ochre) *miaD*::mini-Tn*10*(Km^r)	DEV15 *su*$^+$*9 miaA* × P1 *kc* (NU1552)

[a] Several additional strains from the mapping kit assembled by Singer et al. (41) are described in Table 3.

[b] Antibiotic resistances: Tc, tetracycline; Km, kanamycin.

[c] Since publication of reference 15, we found that the W3110 strain, NU426, which we have used as a prototrophic genetic background contains a cryptic amber suppressing activity. However, the DEV15 and NU753 background used to measure the *miaA* mutator phenotype lack detectable amber suppression based on their inability to act as hosts for lambda amber mutants (data not shown). NU814, which also lacks detectable suppressor activity, replaces NU426 as our prototrophic genetic background.

[d] KmSma and KmΔMlu designate chromosomal kanamycin cassette (Km^r) insertions and insertion-deletions in the *Sma*I site of *miaA* and between the *Mlu*I sites upstream and presumably in *mutL*, respectively (Fig. 2) (15).

*Bam*HI site in *miaA* has already been determined on both strands (15). To complete the DNA sequence of the new clones, we synthesized five oligonucleotides. Oligonucleotides 1, 2, and 5 had the same sequences as the coding strand and extended from positions 3 to 22, 699 to 718, and 965 to 983, respectively (Fig. 3). Oligonucleotides 3 and 4 corresponded to positions 965 to 983 and 678 to 696, respectively, of the noncoding strand. Each segment of the DNA sequence was determined with the Sequenase-dITP, Sequenase-dGTP, and Klenow-deaza-dGTP variations of the Sanger dideoxynucleotide method as described previously (15). Sequence data were analyzed by using the UWGCG (University of Wisconsin, Madison) and PCGene (Intelligenics, Inc., Mountain View, Calif.) computer programs.

Amounts of *miaA* gene transcripts were determined in exponentially growing bacteria by an RNase T2 mapping protocol with labeled antisense RNA probes as described before (15).

Nucleotide sequence accession number. The GenBank accession number is M37459.

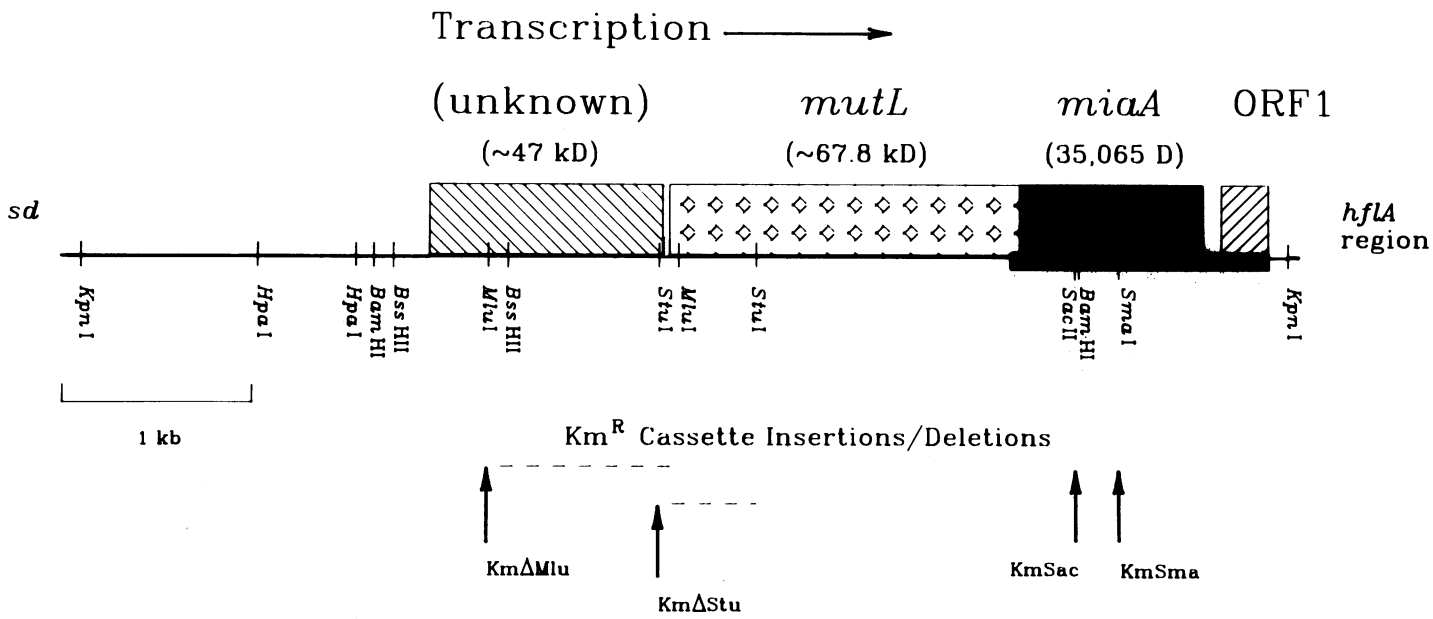

FIG. 2. Structure of the complex *mutL-miaA* operon. The figure is drawn to scale. The region corresponding to the DNA sequence reported here is indicated by the heavy black line at the right. Evidence that *miaA* and *mutL* are in the same operon is presented in the text. Previous work in *E. coli* and *S. typhimurium* suggests that the operon contains at least one additional gene that encodes a 47-kDa polypeptide (see text) (15, 27, 35). Placements of *mutL* and the gene encoding the 47-kDa polypeptide are approximated based on the *S. typhimurium* DNA sequence (27). It is not known whether downstream ORF1 is part of the operon or whether ORF1 corresponds to *hflX*, which is very close to *miaA* (4). Positions of chromosomal kanamycin cassette (Km^r) insertions and insertion-deletions reported previously are shown (see text [15]).

RESULTS

DNA sequence of *E. coli* K-12 *miaA*. Previously we cloned and determined the approximate locations of *E. coli* K-12 *miaA*, *mutL*, and a gene encoding a 47-kDa polypeptide in the *Bss*HII-*Kpn*I fragment at the right of the larger *Kpn*I-*Kpn*I fragment depicted in Fig. 2. At that time, we completed only a limited DNA sequence between the *Bam*HI-*Sma*I sites to demonstrate that this fragment was contained within the *miaA* coding region and could be used to probe *miaA* mRNA levels (15). Chromosomal insertion of a kanamycin resistance cassette (Km^r) into the *Sma*I site (KmSma, Fig. 2) inactivated *miaA*, whereas insertion of a double cassette into the *Sac*II site immediately upstream from the *Bam*HI site (KmSac, Fig. 2) failed to inactivate *miaA* (15). However, the KmSac double insertions behaved aberrantly in that they did not show the same polarity on *miaA* transcription as insertions further upstream between the *Mlu*I sites (KmΔMlu, Fig. 2). The KmΔMlu insertions inactivated *mutL* and reduced steady-state levels of *miaA* mRNA four- to eightfold, depending on the orientation of the Km^r cassette (15).

To localize *miaA* exactly, we determined the DNA sequence for the region indicated by the heavy black line in Fig. 2. The DNA sequence (Fig. 3) contained the end of the *mutL* coding region, the entire *miaA* gene, a potential intercistronic region of 86 nucleotides, and the beginning of another relatively long open reading frame (ORF1). We assigned the end of *mutL* based on the published *Salmonella typhimurium mutL* sequence reported by Mankovich and coworkers (27). We identified the MiaA coding region by the extensive number of amino acids matches with yeast Mod5 (Fig. 4) (32). MiaA and Mod5 have similar amino acid sequences over the entire length of the MiaA open reading frame.

Both MiaA (amino acids 206 to 233, SRELLHQRIEQR FHQMLASGFEAE) and Mod5 (amino acids 210 to 232, PEPLFQRLDDRVDDMLERGALQE) contain domain 1 isopentenylpyrophosphate substrate binding sites found in farnysyl pyrophosphate synthetase and other prenyl synthetases (2a). Interestingly, the Mod5 enzyme extends an additional 92 amino acids, which suggests that it has a second functional domain and enzymatic activity. The smaller size of MiaA predicted from the DNA sequence compared with Mod5 is consistent with the ≈34,000-Da subunit molecular mass of MiaA expressed in minicells (15). Because the apparent molecular mass of native MiaA transferase is about 55,000 Da (5), the active enzyme is probably a dimer of identical subunits.

There are two putative translation starts for *miaA* at position 56 or 101 (Fig. 3). We favor the start at position 56 for three reasons. First, comparison between the *E. coli* MiaA and yeast Mod5 sequences (Fig. 4) reveals that conserved amino acids are present before AUG(101), which suggests that the upstream AUG at position 56 is used to initiate translation. Second, the partial sequence of *S. typhimurium miaA*, which was determined along with *mutL* (27), shows extensive conservation at the base and amino acid levels with the *E. coli* sequences between the putative translation start points (Fig. 3 and 4). If AUG(101) was used to initiate translation, then this region would be an intercistronic region. Based on a limited number of examples, long intercistronic regions show considerable divergence between *E. coli* and *S. typhimurium* (e.g., *trpC-trpB* [40, 47]), which again favors the start at AUG(56). Third, neither putative translation start is preceded by a good Shine-Dalgarno sequence; however, AUG(56) overlaps the last two codons of *mutL*, which could allow translational coupling between *mutL* and *miaA* (23). Finally, as noted above, translation initiation at Aug(56) or AUG(101) would result in

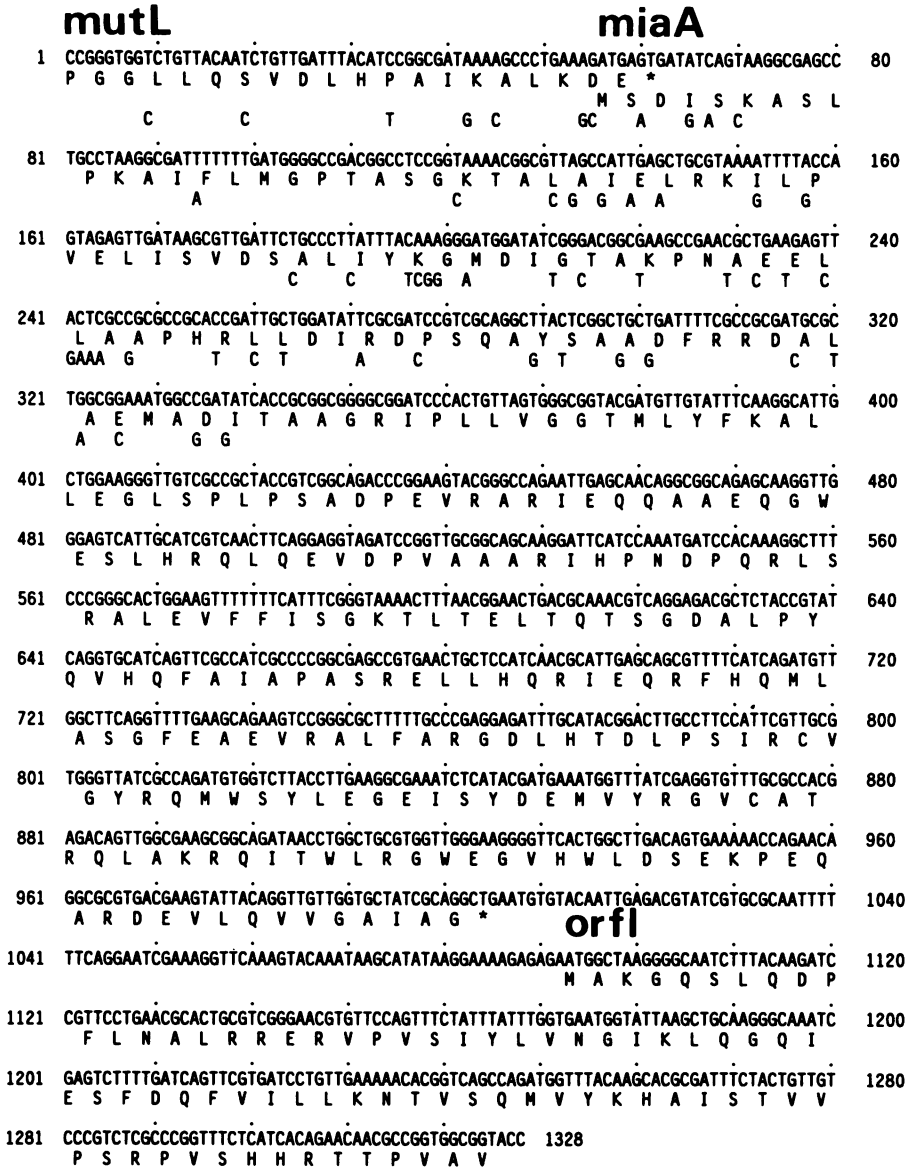

FIG. 3. DNA sequence of *E. coli* K-12 *miaA*. The end of *mutL*, the *miaA* reading frame, and ORF1 are marked. The strategy and details about the sequence are discussed in the text. Bases below the *E. coli* sequence show differences with the *S. typhimurium* DNA sequence, which extends to position 340 (27).

polypeptides with molecular masses of 35,065 or 33,462 Da, respectively, which matches the size of MiaA expressed in minicells (15).

Another interesting structural feature is the presence of a putative ATP/GTP motif A binding site at the same relative position near the amino terminus of each enzyme (MiaA amino acids 17 to 24, GPTASGKT; Mod5 amino acids 21 to 28, GTTGVGKS; Fig. 4) (43). ATP or GTP is not known to be required for the isopentenylpyrophosphate transferase reaction (5). Whether this conserved potential site actually binds nucleotide triphosphates and regulates enzyme activity awaits future biochemical analysis.

The identity of ORF1 and whether it is in the same operon with *miaA* are unknown. There are no strong rho-independent transcription terminator structures in the 86-nucleotide intercistronic region between *miaA* and ORF1, which might mean the two genes are cotranscribed. It is possible that ORF1 corresponds to *hflX*, since the *hflA* region is located extremely close to *miaA* (4).

Mutation spectrum caused by *miaA* insertion mutations. Our previous findings showed that chromosomal Km^r cassette insertions in the *Sma*I (563) site of *miaA* (Fig. 2 and 3) caused a mutator phenotype with a spectrum that appeared to be different from insertions or deletions into the *Stu*I or *Mlu*I sites that must be in *mutL* (Fig. 2) (15). Control experiments established that the *miaA* mutator phenotype was not caused by polarity on downstream gene expression. We wanted to determine the exact mutation spectrum caused by *miaA* mutants. To this end, we used the set of six *lacZ* mutator tester strains developed by Cupples and Miller (16). Each strain contains an F′ *lac-proB*$^+$ episome with a different *lacZ* allele in codon 461. Reversion to Lac$^+$ of each

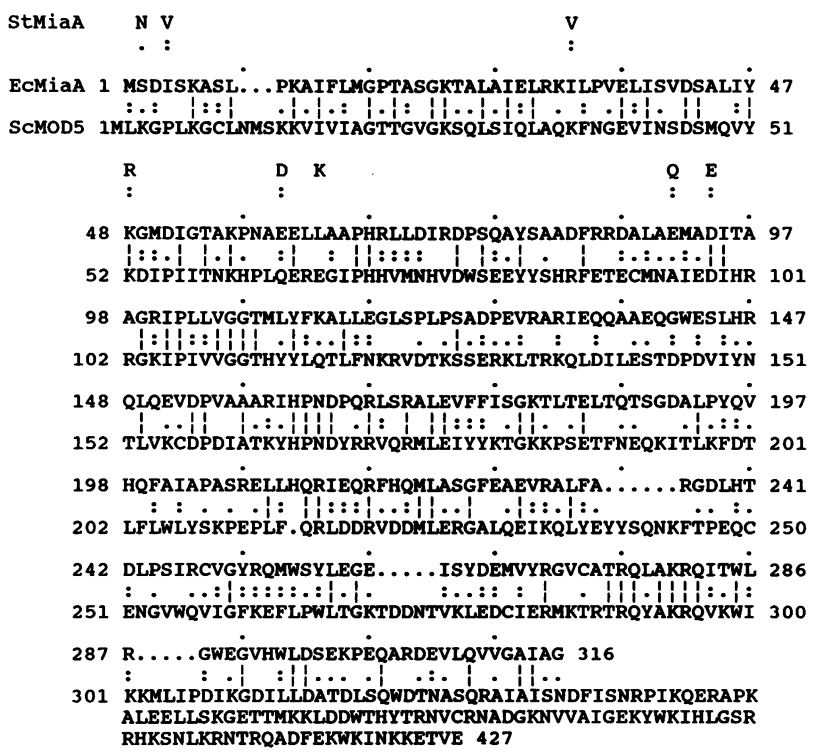

FIG. 4. Comparison between the predicted amino acid sequences of *E. coli* K-12 MiaA (EcMiaA) and yeast Mod5 (ScMOD5 [32]). Structural similarities and differences are considered in the text. Amino acids above the *E. coli* sequence show differences deduced from the partial *S. typhimurium* DNA sequence (StMiaA; Fig. 3) (27).

tester strain can only occur by a specific base substitution that restores codon 461 to encode glutamic acid.

The *miaA*::KmSma insertion specifically caused GC→TA transversion mutations at higher frequency (approximately sixfold) than its isogenic *miaA*$^+$ parent (Table 2). This spectrum and magnitude are consistent with reversion of *lacZ*(UGA) (29-fold) and *trpA46PR9* (11-fold) alleles used previously to quantitate the *miaA* mutator phenotype (15). By contrast, the *mutL*::KmΔMlu insertion-deletion caused mainly GC→AT and AT→GC transition mutations (Table 2), which was expected from earlier reports (39). The GC→TA transversions caused by the *mutL*::KmΔMlu mutation were probably due to polarity on *miaA* expression, since we showed previously that transcription of *miaA* is reduced significantly by the upstream *mutL*::KmΔMlu insertion-deletion (15). Thus, the results shown in Table 2 support the contention that the *miaA* and *mutL* mutator phenotypes are distinct.

The *miaA* mutator phenotype was also characterized in two additional ways. Strain NU1514 (CC104 *miaA*::Km^r) formed numerous blue Lac$^+$ papillae on the minimal (A) salts–0.2% (wt/vol) glucose–40 μg of X-Gal (5-bromo-4-chloro-3-indolyl-β-D-galactoside) per ml–0.05% (wt/vol) P-Gal (phenyl-β-D-galactoside) medium devised by Nghiem et al. (33) to screen for mutator strains (data not shown). Papillation in the CC104 background indicated GC→TA transversions to Lac$^+$ and was consistent with Table 2, although the growth conditions allowing visualization of the *miaA* mutator phenotype are quite different in the two experiments. The *miaA*::Km^r mutation did not increase papillation of the other mutator tester strains compared with their parent strains (data not shown), which is again consistent with Table 2.

We tested for the *miaA* mutator phenotype using one other growth condition. It has been observed that *miaA* mutants grow slower than *miaA*$^+$ strains on the minimal salts plus

TABLE 2. Reversion frequencies of specific *lacZ* mutations in Cupples-Miller tester strains containing *miaA*::Km^r and *mutL*::Km^r insertion mutations

Mutation	Tester strain[a] and reversion event[b]					
	CC101, AT→CG	CC102, GC→AT	CC103, GC→CG	CC104, GC→TA	CC105, AT→TA	CC106, AT→GC
None (*miaA*$^+$ *mutL*$^+$)	<0.5	3.5	<0.5	2.6	2.3	<0.5
miaA::KmSma	<0.5	2.1	<0.5	16.7	1.7	<0.5
mutL::KmMlu	<0.5	195	<0.5	7.6	2.4	34.5

[a] Strains CC101 to CC106 and NU1505 to NU1521 (Table 1).

[b] Strains were grown overnight in LBC medium at 37°C with shaking. Cells were collected by centrifugation, washed, and resuspended in minimal salts (E) medium (MM) lacking a carbon source. Aliquots of washed cells were spread onto MM plus 0.4% glucose plates to measure episome retention and MM plus 0.4% lactose plates to measure *lac*$^+$ reversion. The plates were incubated at 37°C for 2 to 4 days before scoring. Results are expressed as *lac*$^+$ revertants per 10^8 *proB*$^+$ cells. The entire experiment was repeated several times, and standard deviations of the mean were less than 12% for CC104 *miaA*$^+$ and CC104 *miaA*::KmSma.

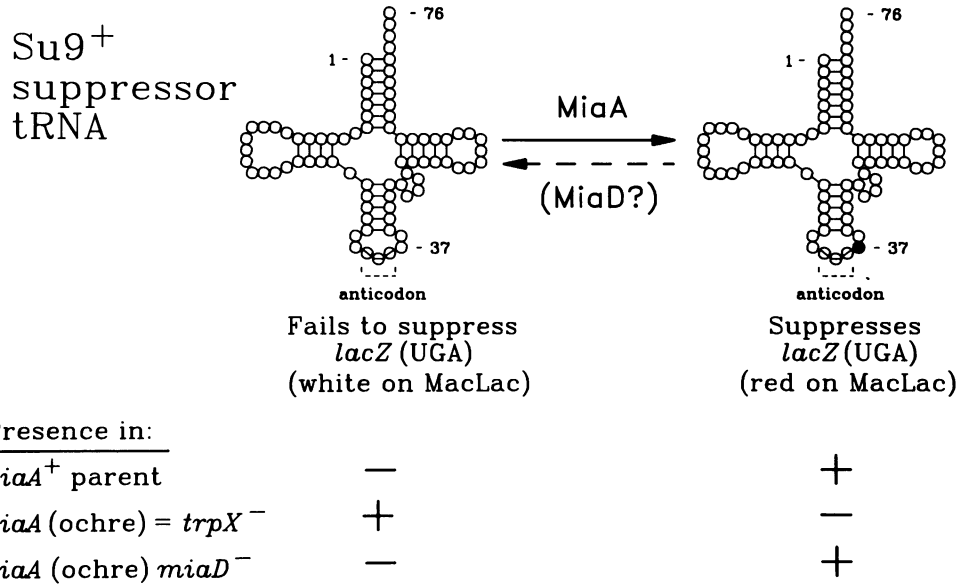

FIG. 5. Screening strategy for *miaD*::mini-Tn*10* suppressor mutations of the leaky *miaA*(ochre) (*trpX*) mutation. The strategy is detailed in Results. MacLac, MacConkey-lactose.

sugar media used to measure reversion frequencies (21). Consequently, it is possible that an apparent mutator phenotype arises because the *miaA*::Km^r mutants spend more time on the selection plates before growth ceases and the greater time allows more chance for spontaneous mutations to occur. The specificity of the *miaA* mutation spectrum and the papillation test described above make this explanation extremely unlikely. Nevertheless, we sought a growth condition in which *miaA*::Km^r mutants grow faster than their *miaA*$^+$ parents. We found that *miaA*::Km^r mutants utilize several amino acids, notably proline, and tricarboxylic acid cycle intermediates better than *miaA*$^+$ strains, and consequently, *miaA*::Km^r mutants grow faster than their *miaA*$^+$ parents on minimal medium (MM) supplemented with acid casein hydrolysate as a primary carbon source (14a). When we measured reversion frequency of the *trpA46PR9* allele to Trp$^+$ on MM plus acid casein hydrolysate at 37°C, we found that the *miaA*::Km^r mutant still reverted 10- to 12-fold more than its isogenic *miaA*$^+$ parent (data not shown). Together, these findings verify that lesions in *miaA* increase the spontaneous mutation frequency 6- to 30-fold, depending on the context of the mutation used to measure reversion.

Isolation of *miaD* suppressors of the *miaA*(ochre) (*trpX*) mutation. We wanted further to confirm that the presence of the ms^{2}i^{6}A-37 tRNA modification was directly correlated with the changes in spontaneous mutation frequency described above and before (15). At the same time, we wanted to examine genetically whether tRNA demodification or regulation of the *miaA* gene might be occurring in vivo. To these ends, we devised a strategy to select for suppression of a somewhat leaky *miaA*(ochre) mutation, designated the *trpX* allele (Fig. 5) (20, 37). The *miaA*(ochre) mutation leaks enough so that about 5 to 16% of the ms^{2}i^{6}A-37 normally present in the tRNA of *miaA*$^+$ strains accumulates in the mutant (42). This level cannot be detected by standard HPLC methods used to measure modified bases (Fig. 6A), and function of specific suppressor tRNAs, such as Su$^+$9, is impaired in the *miaA*(ochre) mutant (Fig. 5). We reasoned that if demodification occurs and can be blocked or if *miaA* gene expression is regulated and can be increased, then we would be able to isolate an insertion mutation (designated *miaD*) that accumulates ms^{2}i^{6}A-37-modified tRNA in the *miaA*(ochre) mutant background (Fig. 5). We also predicted that a *miaD* mutation would restore spontaneous mutation frequencies to a *miaA*(ochre) mutant characteristic of a *miaA*$^+$ strain.

We isolated a putative *miaD*::mini-Tn*10* mutant by jumping mini-Tn*10*(Km^r) elements randomly into the chromosome of a *lacZ*(UGA) Su$^+$9 *miaA*(ochre) mutant that normally forms white colonies with faint pink centers on MacConkey-lactose agar at 37°C (Fig. 5). We then screened for dark red colonies on MacConkey-lactose-kanamycin agar at 37°C. One candidate was isolated from screening about 2,500 Km^r colonies.

Several criteria ruled out that the *miaD*::mini-Tn*10* mutation was in the *lac* or *mutL-miaA* operon. First, the *miaD*::mini-Tn*10* mutation restored about 80% of the ms^{2}i^{6}A-37 tRNA modification to a *miaA*(ochre) mutant (Fig. 6), which makes it unlikely that it is affecting *lac* operon expression or amounts of suppressor tRNA. By contrast, the *miaD*::mini-Tn*10* mutation did not restore the ms^{2}i^{6}A-37 tRNA modification to a *miaA*::Tn*10*(Tc^r) knockout mutation (HPLC not shown), which is consistent with the screening scheme (Fig. 5). Second, the mini-Tn*10*(Km^r) insertion mapped to 99.75 min on the *E. coli* chromosome (Table 3), which is distant from both *miaA* at 95 min and *lac* at 8 min. Last, the *miaD*::mini-Tn*10* mutation did not seem to have a general effect on ochre codon suppression, since it did not suppress *lacZ*(UAA) mutations in two different genetic backgrounds (NU1847 and NU1848; data not shown).

Taken together, these results suggest that *miaD* represents a unique locus that either decreases ms^{2}i^{6}A-37 demodification or increases *miaA* gene expression. We tested whether *miaD*::mini-Tn*10*(Km^r) increases *mutL-miaA* operon transcription by measuring steady-state levels of *miaA* transcripts in isogenic strains DEV15 (*su*$^+$*9 miaA*$^+$ *miaD*$^+$) and NU1887 [DEV15 *su*$^+$*9 miaA*$^+$ *miaD*::mini-Tn*10*(Km^r)]. Both strains were grown exponentially in LBC medium at 37°C

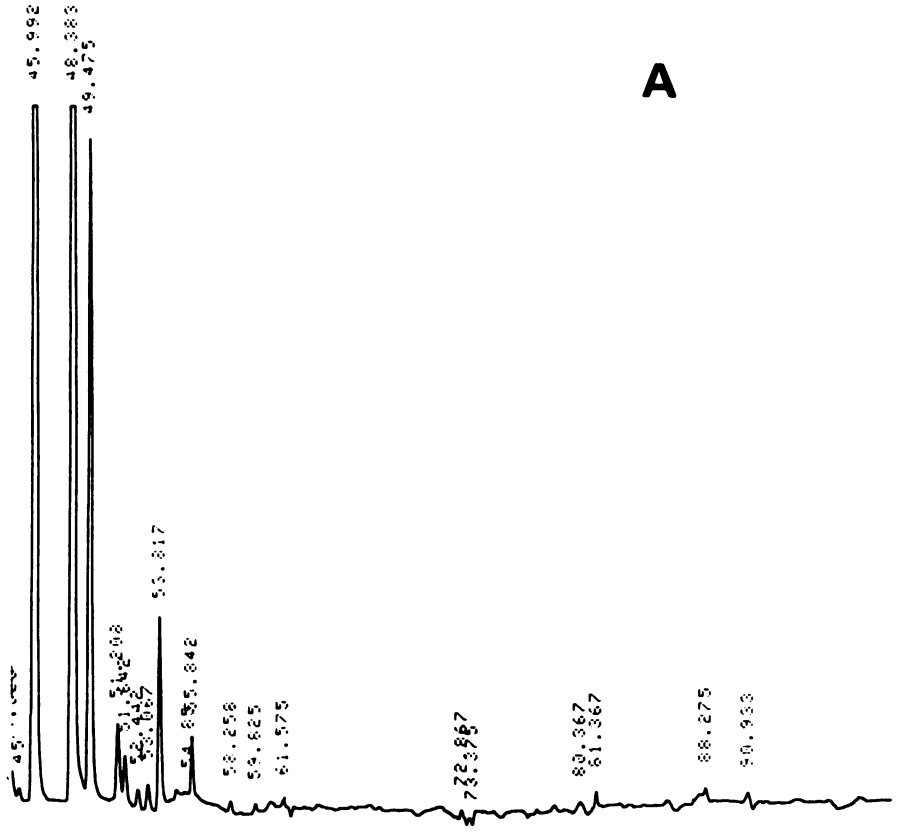
A
45.992
48.383
49.475
53.817
58.258
59.625
61.575
80.367
81.367
88.275
90.933

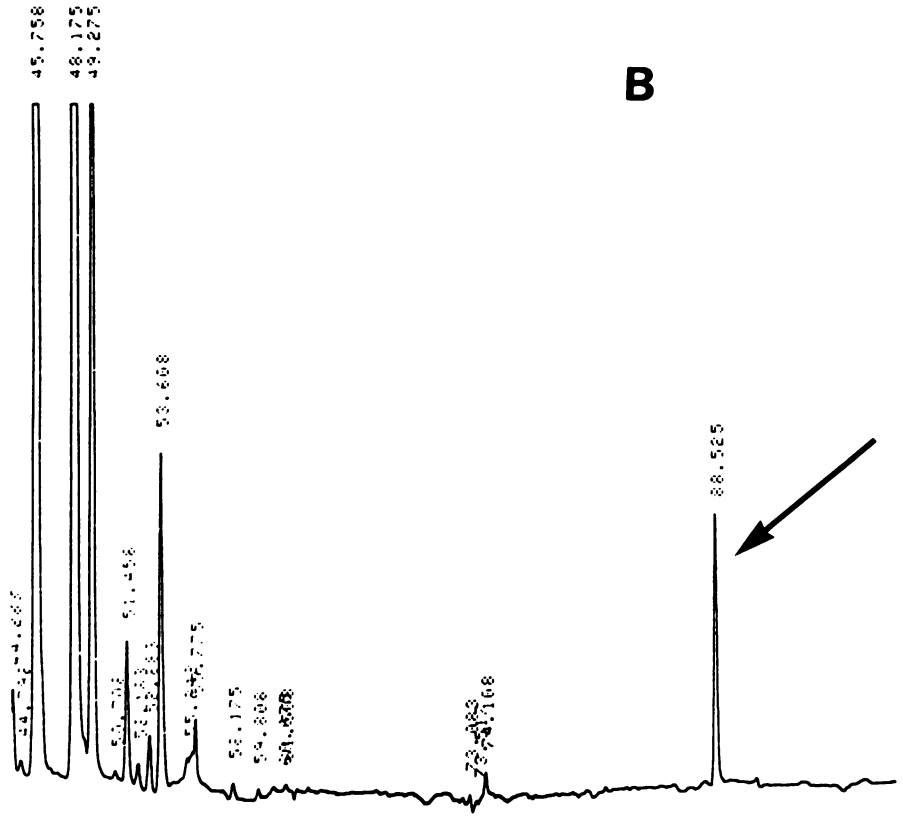
B
45.758
48.175
49.275
53.608
58.175
59.806
88.525

TABLE 3. Mapping of *miaD*::mini-Tn*10*(Km^r)[a]

Tc^r recipient[b]	Location of Tc^r marker (min)	No. of transductants		Approximate cotransduction frequency (%)
		Km^r	Tc^s	
CAG18429	98.25	50	1	2
CAG18430	99.5	50	26	52
CAG18494	99.75	50	34	68
CAG18422	0	50	27	54
CAG12093	0.75	50	15	30

[a] Preliminary Hfr mapping was performed by the method of Singer et al. (41) and localized the *miaD*::mini-Tn*10*(Km^r) insertion to 70 to 100 min on the *E. coli* K-12 chromosome (data not shown). More exact mapping was completed by generalized P1 phage transduction (Materials and Methods) (30). P1 *kc* phage were propagated on strain NU1552 and used to infect the indicated strains from the mapping kit assembled by Singer et al. (41). Kanamycin-resistant (Km^r) transductants were selected on LBC medium containing 50 μg of kanamycin per ml at 37°C. Fifty transductants from each cross were then scored for loss of tetracycline resistance on LBC plates containing 10 μg of tetracycline per ml at 37°C. The transduction experiment was performed twice with similar results. No Km^r Tc^s transductants were generated in crosses with recipients whose Tc^r markers are located between 70 and 98 min (data not shown).

[b] Donor is NU1552 [*miaD*::mini-Tn*10*(Km^r)].

TABLE 4. Properties of strains containing *miaA*::KmSma and *miaD*::mini-Tn*10*(Km^r) mutations

Mutation	*su*$^+$*9* function[a]	Mutator phenotype[b]	Doubling time (min)[c] in:	
			LBC	MMG
None (*miaA*$^+$ *miaD*$^+$)	+	−	29	90
miaA(ochre) = *trpX*	−	+	41	126
miaD::mini-Tn*10*(Km^r)	+	−	ND[d]	93
miaA(ochre) *miaD*::mini-Tn*10*(Km^r)	+	−	30	87

[a] Determined in the DEV15 *su*$^+$*9* background (strains DEV *su*$^+$*9*, DEV15 *su*$^+$*9 miaA*, NU1887, and NU1888 [Table 1]) as described in Materials and Methods.

[b] Determined by reversion to Lac$^+$ in the DEV15 background (strains DEV15, DEV15 *miaA*, NU1885, and NU1879 [Table 1]) as described in Materials and Methods.

[c] Determined for the DEV15 genetic background (see footnote *b*, above) in liquid cultures with vigorous shaking at 37°C.

[d] ND, Not determined.

with shaking. When cultures reached 70 Klett units, total RNA was purified as described previously (15). The total RNA was hybridized to a radioactively labeled *miaA*-specific RNA probe corresponding to the region between *Sac*II (345) and *Sma*I (563) in Fig. 3. Hybrids were digested with RNase T2, and full-length protected probe corresponding to *miaA* transcripts was resolved on formamide-urea denaturing gels (15). By this analysis, the amount of steady-state *miaA* transcript was the same within experimental error from the *miaD*$^+$ and *miaD*::mini-Tn*10*(Km^r) strains (data not shown). Thus, the *miaD*::mini-Tn*10*(Km^r) mutation does not appear to increase *mutL-miaA* operon transcription. However, it is still possible that *miaD*::mini-Tn*10*(Km^r) could be increasing *miaA* expression posttranscriptionally.

Table 4 shows that by restoring the ms^{2}i^{6}A-37 tRNA modification in the *miaA*(ochre) mutant, the *miaD*::mini-Tn*10* mutation simultaneously restores Su$^+$9 suppressor tRNA function, decreases cellular doubling time back to the rate characteristic of the *miaA*$^+$ parent, and abolishes the *miaA* mutator phenotype. The last observation is particularly significant, because it directly correlates the presence of the ms^{2}i^{6}A-37 tRNA modification with the appearance of the mutator phenotype. This conclusion supports the idea that change in the level of the ms^{2}i^{6}A-37 tRNA modification acts as a physiological switch to modulate spontaneous mutation frequency and possibly other metabolic functions (see Discussion) (9, 15).

DISCUSSION

In this report, we show that *miaA* is extremely close to *mutL* (Fig. 2 and 3). In fact, the most likely translational start codon of *miaA* overlaps the last two codons of *mutL*, which suggests that there is translational coupling between the expression of *mutL* and *miaA* (Fig. 3). Together with earlier results showing that upstream insertions in *mutL* are polar on *miaA* transcription in vivo, their close proximity confirms that *mutL* and *miaA* are in the same complex operon. Previous data from both *E. coli* and *S. typhimurium* suggest that the *mutL-miaA* operon contains at least one additional upstream gene that encodes a 47-kDa polypeptide of unknown function (Fig. 2) (15, 27, 35). The DNA sequence presented here implies that the *mutL-miaA* operon contains downstream genes as well (Fig. 2 and 3). It is known that the three-gene *hflA* region is extremely close to *miaA* (4), and ORF1 in Fig. 2 and 3 may represent the start of *hflX*.

Our previous mutational analysis showed that insertions of Km^r cassettes into the *Sma*I (563) but not the *Sac*II (345) site inactivated *miaA* (Fig. 2 and 3) (15). Based on the DNA sequence, the KmSac (345) double-cassette insertion clearly should have knocked out *miaA*. At the time, we noted the anomalous lack of polarity of the KmSac insertions on *miaA* transcription (2, 15). Perhaps the KmSac insertions recombined aberrantly into the bacterial chromosome outside of the *miaA-mutL* operon. However, P1 cotransductional analysis of the KmSac insertion showed that the Km^r marker was 100% cotransducible with a *miaA*::Tn*10*(Tc^r) mutation, so an aberrant crossover had to occur very close to *miaA* (data not shown). Alternatively, a fusion protein might have been formed in the KmSac constructions that retains sufficient MiaA function to give positive results in the phenotypic tests used before (15). This explanation would account for complementation of *miaA* mutations by plasmids containing KmSac insertions (15). Further Southern and DNA sequence analyses are required to explain the anomalous behavior of the "KmSac" mutations.

We speculated previously that *mutL* and *miaA* were grouped together in a complex operon, because both genes could play roles in setting spontaneous mutation frequency (15). The earlier work also suggested that the spontaneous mutation spectra observed for *miaA* and *mutL* mutants were apparently different. We confirm this conclusion here. Insertions in *mutL* cause primarily GC→AT and AT→GC transitions, whereas insertions in miaA cause exclusively

FIG. 6. HPLC analysis of nucleosides contained in total cellular RNA isolated from strains DEV15 *su*$^+$*9 miaA*(ochre) (A) and NU1552 [DEV15 *su*$^+$*9 miaA*)(ochre) *miaD*::mini-Tn*10*(Km^r)] (B). Bacteria were grown in LBC medium with shaking at 37°C, and total RNA was isolated, digested to nucleosides, and analyzed by LC-18-S column reverse-phase HPLC as described before (15). The prominent peak at 88.525 min in panel B (arrow), which is absent from panel A, corresponds to ms^{2}i^{6}A.

GC→TA transversions (Table 2). Thus, *mutL* and *miaA* seem to affect different mutagenesis pathways. To date, only *mutY* and *mutM* mutations have been observed exclusively to cause GC→TA transversions in *E. coli* (12, 33). The *mutY* gene encodes an adenine DNA glycosylase that is active in methyl-independent G-A to G-C mismatch repair (3, 29). The function of *mutM* is unknown, but it may participate in the same repair pathway as *mutY* (12). The fact that *miaA* mutations also cause GC→TA transversions might mean that MutY or MutM amount or activity is decreased by ms^2i^6A-37 tRNA undermodification. Of course, other explanations for the *miaA* mutator phenotype are possible, such as changes in nucleotide triphosphate pools caused by defective attenuation of pyrimidine or purine biosynthetic operons (38). Perhaps the slower translation per se caused by ms^2i^6A-37 tRNA undermodification (21) signals for the higher spontaneous mutation frequency observed in *miaA* mutants and iron-limited *miaA*$^+$ cells (15). These hypothetical targets will be tested in future experiments.

In this paper, we also report the isolation of a novel suppressor locus, designated *miaD*, of the leaky *miaA* (ochre) (*trpX*) mutation (Fig. 5 and 6; Tables 3 and 4). From the screening strategy (Fig. 5) and in view of the experiments described in the Results, it is possible that the *miaD* mutation decreases ms^2i^6A-37 demodification or increases post-transcriptional expression of the *miaA* gene. Either explanation would lead to accumulation of fully modified tRNA in the *miaA*(ochre) mutant (Fig. 5). Nothing is firmly established about the turnover of modified bases in tRNA molecules or whether active demodification occurs. One report suggests that demodification of i^6A-37 occurs in bacterial and rat liver cellular extracts (28); however, the data are very preliminary. If demodification of ms^2i^6A-37 does take place, then the level of tRNA modification could act as an active physiological switch to regulate sets of genes in response to growth condition. Preliminary experiments show that carbon limitation of *miaA*$^+$ *E. coli* leads to at least a fourfold drop in the amount of ms^2i^6A relative to other modified bases found exclusively in tRNA molecules (14a). Such a decrease is consistent with in vivo demodification of ms^2i^6A-37 in tRNA. On the other hand, little is known about the regulation of the *mutL-miaA* operon, other than that *miaA* transcription is significantly induced by 2-aminopurine (15). Therefore, further analysis of *miaD* function might lead to important new insights into tRNA demodification or regulation of *miaA* in the complex *mutL-miaA* operon.

ACKNOWLEDGMENTS

We thank D. Elseviers, C. Gross, N. Kleckner, J. Miller, and C. Yanofsky for bacterial strains and phage, J. Miller for information about mutator tester strains, and D. Womble and R. Rownd for help with completion of this work.

This work was initially supported from Public Health Service grant GM37561 and continued with support from grant GM43070 from the National Institute of General Medical Sciences to M.W. D.M.C. was a trainee on Public Health Service grant GM08061 for part of the time it took to complete this research.

REFERENCES

1. **Agris, P. F., D. J. Armstrong, K. P. Schäfer, and D. Söll.** 1975. Maturation of a hypermodified nucleoside in transfer RNA. Nucleic Acids Res. **2**:691–698.
2. **Arps, P. J., and M. E. Winkler.** 1987. Structural analysis of the *Escherichia coli* K-12 *hisT* operon by using a kanamycin resistance cassette. J. Bacteriol. **169**:1061–1070.

2a. **Ashby, M., and P. Edwards.** Personal communication.

3. **Au, K. G., S. Clark, J. H. Miller, and P. Modrich.** 1989. *Escherichia coli mutY* gene encodes an adenine glycosylase active on G-A mispairs. Proc. Natl. Acad. Sci. USA **86**:8877–8881.
4. **Banuett, F., and I. Herskowitz.** 1987. Identification of polypeptides encoded by an *Escherichia coli* locus (*hflA*) that governs the lysis-lysogeny decision of bacteriophage lambda. J. Bacteriol. **169**:4076–4085.
5. **Bartz, J. K., L. K. Kline, and D. Söll.** 1970. N^6-(2-isopentenyl) adenosine: biosynthesis *in vitro* in transfer RNA by an enzyme purified from *Escherichia coli*. Biochem. Biophys. Res. Commun. **40**:1481–1487.
6. **Björk, G. R.** 1987. Modification of stable RNA, p. 719–731. *In* F. C. Neidhardt, J. L. Ingraham, K. B. Low, B. Magasanik, M. Schaechter, and H. E. Umbarger (ed.), *Escherichia coli* and *Salmonella typhimurium*: cellular and molecular biology. American Society for Microbiology, Washington, D.C.
7. **Björk, G. R., J. U. Ericson, C. E. Gustafsson, T. G. Hagervall, Y. H. Jonsson, and P. M. Wikstrom.** 1987. Transfer RNA modification. Annu. Rev. Biochem. **56**:263–287.
8. **Blum, P. H.** 1988. Reduced *leu* operon expression in a *miaA* mutant of *Salmonella typhimurium*. J. Bacteriol. **170**:5125–5133.
9. **Buck, M., and B. N. Ames.** 1984. A modified nucleotide in tRNA as a possible regulator of aerobiosis: synthesis of *cis*-2-methylthioribosylzeatin in the tRNA of *Salmonella*. Cell **36**:523–531.
10. **Buck, M., and E. Griffiths.** 1981. Regulation of aromatic amino acid transport by tRNA: role of 2-methylthio-N^6-(Δ^2-isopentenyl)-adenosine. Nucleic Acids Res. **9**:401–414.
11. **Buck, M., and E. Griffiths.** 1982. Iron mediated methylthiolation of tRNA as a regulator of operon expression in *Escherichia coli*. Nucleic Acids Res. **10**:2609–2624.
12. **Cabrera, M., Y. Nghiem, and J. H. Miller.** 1988. *mutM*, a second mutator locus in *Escherichia coli* that generates GC→TA transversions. J. Bacteriol. **170**:5405–5407.
13. **Caillet, J., and L. Droogmans.** 1988. Molecular cloning of the *Escherichia coli miaA* gene involved in the formation of Δ2-isopentenyl adenosine in tRNA. J. Bacteriol. **170**:4147–4152.
14. **Choy, H. E., and R. G. Fowler.** 1985. The specificity of base-pair substitution induced by the *mutL* and *mutS* mutators in *E. coli*. Mutat. Res. **142**:93–97.

14a. **Connolly, D., and M. Winkler.** Unpublished observation.

15. **Connolly, D. M., and M. E. Winkler.** 1989. Genetic and physiological relationships among the *miaA* gene, 2-methylthio-N^6-(Δ^2-isopentenyl)adenosine tRNA modification, and spontaneous mutagenesis in *Escherichia coli* K-12. J. Bacteriol. **171**:3233–3246.
16. **Cupples, C. G., and J. H. Miller.** 1989. A set of *lacZ* mutations in *Escherichia coli* that allow rapid detection of each of the six base substitutions. Proc. Natl. Acad. Sci. USA **86**:5345–5349.
17. **Davis, R. W., D. Botstein, and J. R. Roth.** 1980. Advanced bacterial genetics. Cold Spring Harbor Laboratory, Cold Spring Harbor, N.Y.
18. **Dihanich, M. E., D. Najarian, R. Clark, E. C. Gillman, N. C. Martin, and A. K. Hopper.** 1987. Isolation and characterization of *mod5*, a gene required for isopentenylation of cytoplasmic and mitochondrial tRNAs of *Saccharomyces cerevisiae*. Mol. Cell. Biol. **7**:177–184.
19. **Echols, H.** 1982. Mutation rate: some biological and biochemical considerations. Biochimie **64**:571–575.
20. **Eisenberg, S. P., M. Yarus, and L. Soll.** 1979. The effect of an *Escherichia coli* regulatory mutation on transfer RNA structure. J. Mol. Biol. **135**:11–126.
21. **Ericson, J. U., and G. R. Björk.** 1986. Pleiotropic effects induced by modification deficiency next to the anticodon of tRNA *Salmonella typhimurium* LT2. J. Bacteriol. **166**:1013–1021.
22. **Gefter, M. L.** 1969. The *in vitro* synthesis of 2′-*O*-methylguanosine and 2-methylthio-^6N(dimethylallyl)adenosine in transfer RNA of *Escherichia coli*. Biochem. Biophys. Res. Commun. **36**:435–441.
23. **Gold, L., and G. Stormo.** 1987. Translational initiation, p. 1302–1307. *In* F. C. Neidhardt, J. L. Ingraham, K. B. Low, B. Magasanik, M. Schaechter, and H. E. Umbarger (ed.), *Escherichia coli* and *Salmonella typhimurium*: cellular and molecular

biology. American Society for Microbiology, Washington, D.C.
24. **Gowrishankar, J., and J. Pittard.** 1982. Regulation of phenylalanine biosynthesis in *Escherichia coli* K-12: control of transcription of the *pheA* operon. J. Bacteriol. **150**:1130–1137.
25. **Griffiths, E., and J. Humphreys.** 1978. Alterations in tRNAs containing 2-methylthio-N^6-(Δ^2-isopentenyl)-adenosine during growth of enteropathogenic *Escherichia coli* in the presence of iron binding proteins. Eur. J. Biochem. **82**:503–513.
26. **Lu, A. L., S. Clark, and P. Modrich.** 1983. Methyl-directed mismatch repair of DNA base-pair mismatches *in vitro*. Proc. Natl. Acad. Sci. USA **80**:4639–4643.
27. **Mankovich, J. A., C. A. McIntyre, and G. C. Walker.** 1989. Nucleotide sequence of the *Salmonella typhimurium mutL* gene required for mismatch repair: homology of MutL to HexB of *Streptococcus pneumoniae* and to PMS1 of the yeast *Saccharomyces cerevisiae*. J. Bacteriol. **171**:5325–5331.
28. **McLennan, B. D.** 1975. Enzymatic demodification of transfer RNA species containing N^6-(Δ^2-isopentenyl)adenosine. Biochem. Biophys. Res. Commun. **65**:345–351.
29. **Michaels, M. L., L. Pham, Y. Nghiem, C. Cruz, and J. H. Miller.** 1990. MutY, an adenine glycosylase active on G-A mispairs, has homology to endonuclease III. Nucleic Acids Res. **18**:3841–3845.
30. **Miller, J. H.** 1972. Experiments in molecular genetics. Cold Spring Harbor Laboratory, Cold Spring Harbor, N.Y.
31. **Modrich, P.** 1989. Methyl-directed DNA mismatch correction. J. Biol. Chem. **264**:6597–6600.
32. **Najarian, D., M. E. Dihanich, N. C. Martin, and A. K. Hopper.** 1987. DNA sequence and transcript mapping of *mod5*: features of the 5′ region which suggest two translational starts. Mol. Cell. Biol. **7**:185–191.
33. **Nghiem, Y., M. Cabrera, C. G. Cupples, and J. H. Miller.** 1988. The *mutY* gene: a mutator locus in *Escherichia coli* that generates G:C-A:T transversions. Proc. Natl. Acad. Sci. USA **85**: 2709–2713.
34. **Palmer, D. T., P. H. Blum, and S. W. Artz.** 1983. Effects of the *hisT* mutation of *Salmonella typhimurium* on translation elongation rate. J. Bacteriol. **153**:357–363.
35. **Pang, P. P., A. S. Lundberg, and G. C. Walker.** 1985. Identification and characterization of the *mutL* and *mutS* gene products of *Salmonella typhimurium* LT2. J. Bacteriol. **163**:1007–1015.
36. **Petrullo, L. A., and D. Elseviers.** 1986. Effect of a 2-methylthio-N^6-isopentenyladenosine deficiency on peptidyl-tRNA release in *Escherichia coli*. J. Bacteriol. **165**:608–611.
37. **Petrullo, L. A., P. J. Gallagher, and D. Elseviers.** 1983. The role of 2-methylthio-N^6-isopentenyladenosine in readthrough and suppression of nonsense codons in *Escherichia coli*. Mol. Gen. Genet. **190**:289–294.
38. **Roland, K. L., C. Liu, and C. L. Turnbough.** 1988. Role of the ribosome in suppressing transcriptional termination at the *pyrBI* attenuator of *Escherichia coli* K-12. Proc. Natl. Acad. Sci. USA **85**:7149–7153.
39. **Schaaaper, R. M., and R. L. Dunn.** 1987. Spectra of spontaneous mutations in *Escherichia coli* strains defective in mismatch correction: the nature of *in vivo* DNA replication errors. Proc. Natl. Acad. Sci. USA **84**:6220–6224.
40. **Selker, E., and C. Yanofsky.** 1979. Nucleotide sequence of the *trpC-trpB* intercistronic region from *Salmonella typhimurium*. J. Mol. Biol. **130**:135–143.
41. **Singer, M., T. A. Baker, G. Schnitzler, S. M. Deischel, M. Goel, W. Dove, K. J. Jaacks, A. D. Grossman, J. W. Erickson, and C. A. Gross.** 1989. A collection of strains containing genetically linked alternating antibiotic resistance elements for genetic mapping of *Escherichia coli*. Microbiol. Rev. **53**:1–24.
42. **Vold, B. S., J. M. Lazar, and A. M. Gray.** 1979. Characterization of a deficiency of N^6-(Δ^2-isopentenyl)-2-methylthioadenosine in the *Escherichia coli* mutant *trpX* by use of antibodies to N^6-(Δ^2-isopentenyl)adenosine. J. Biol. Chem. **254**:7362–7367.
43. **Walker, J. E., M. Saraste, M. J. Runswick, and N. J. Gay.** 1982. Distantly related sequences of the alpha- and beta-subunits of ATP synthase, myosin, kinases and other ATP-requiring enzymes and a common nucleotide binding fold. EMBO J. **1**:945–951.
44. **Way, J. C., M. A. Davis, D. Morisato, D. E. Roberts, and N. Kleckner.** 1984. New Tn10 derivatives for transposon mutagenesis and for construction of *lacZ* operon fusions by transposition. Gene **32**:369–379.
45. **Woese, C. R.** 1987. Bacterial evolution. Microbiol. Rev. **51**:221–271.
46. **Yanisch-Perron, C., J. Vieira, and J. Messing.** 1985. Improved M13 phage cloning vectors and host strains: nucleotide sequences of the M13mp18 and pUC19 vectors. Gene **33**:103–109.
47. **Yanofsky, C., T. Platt, I. P. Crawford, B. P. Nichols, G. E. Christe, H. Horowitz, M. VanCleemput, and A. M. Wu.** 1981. The complete nucleotide sequence of the tryptophan operon of *Escherichia coli*. Nucleic Acids Res. **9**:6647–6668.
48. **Yanofsky, C., and L. Soll.** 1977. Mutations affecting $tRNA^{trp}$ and its charging and their effect on regulation of transcription termination at the attenuator of the tryptophan operon. J. Mol. Biol. **113**:663–677.